Journal of Membrane Science 361 (2010) 78–88

Contents lists available at ScienceDirect

Journal of Membrane Science

journal homepage: www.elsevier.com/locate/memsci

Gas transport in membranes based on polynorbornenes with fluorinated dicarboximide side moieties

Joel Vargas [a], Arlette A. Santiago [a], Mikhail A. Tlenkopatchev [b,*], Mar López-González [c,*], Evaristo Riande [c]

[a] Facultad de Química, Universidad Nacional Autónoma de México, CU, Coyoacán, México, DF 04510, Mexico
[b] Instituto de Investigaciones en Materiales, Universidad Nacional Autónoma de México, Apartado Postal 70-360, CU, Coyoacán, México, DF 04510, Mexico
[c] Instituto de Ciencia y Tecnología de Polímeros (CSIC), 28006 Madrid, Spain

ARTICLE INFO

Article history:
Received 26 March 2010
Accepted 2 June 2010
Available online 10 June 2010

Keywords:
Permeation
Sorption
Diffusion
Ring opening metathesis polymerization
Fluorinated polynorbornene dicarboximide

ABSTRACT

This work reports a comparative study of gas transport in membranes based on polynorbornenes and polyoxanorbornenes containing fluorinated dicarboximide side moieties, specifically, poly(*N*-pentafluorophenyl-*exo*-*endo*-norbornene-5,6-dicarboximide), poly(*exo*-*N*-pentafluorophenyl-7-oxanorbornene-5,6-dicarboximide), poly(*N*-3,5-bis(trifluoromethyl)phenyl-*exo*-*endo*-norbornene-5,6-dicarboximide) and a random copolymer of *N*-pentafluorophenyl-*exo*-*endo*-norbornene-5,6-dicarboximide-*co*-*N*-phenyl-*exo*-*endo*-norbornene-5,6-dicarboximide with 50/50 M composition. The gases studied were hydrogen, oxygen, nitrogen, carbon dioxide, methane, ethane, ethylene and propylene. The presence of fluorine atoms in the membranes increases their permeability in slight detriment of the permselectivity, the increase being higher for F–C bonds with carbon hybridization sp^3 than sp^2. The substitution of the CH_2 groups of the norbornene moieties decreases the permeability as a consequence of the decrease of the solubility. A thorough study is carried out on the variation of the permeability coefficient and concentration of condensable gases, such as carbon dioxide and propylene, in the poly(*N*-pentafluorophenyl-*exo*-*endo*-norbornene-5,6-dicarboximide) and poly(*N*-3,5-bis(trifluoromethyl)phenyl-*exo*-*endo*-norbornene-5,6-dicarboximide) membranes finding that the values of the effective diffusion coefficient are similar to those obtained by the dual-mode model but significantly higher than those estimated by the time-lag from permeation results. The results also show that conditioning the membranes with condensable gases under high pressure increases the diffusivity.

1. Introduction

Polynorbornenes are characterized for their excellent dielectric properties in comparison with other materials currently utilized as interlevel dielectrics in electronics [1]. Films prepared from polynorbornes also exhibit rather good gas transport properties which make them suitable materials for their potential use in packaging and gas separation [2]. Studies carried out on the influence of the *cis*/*trans* structures in the transport properties of polynorbornenes obtained by ring opening metathesis polymerization (ROMP) showed that membranes with predominantly *cis* units in the molecular chains exhibit higher permeability than those with predominantly *trans* units [3]. Polynorbornenes present a bonus for the study of gas transport because the chemical structure of this type of polymers can be easily modified thus facilitating the way to prepare homologous functionalized series of polymers in order to find out how slight differences in chemical structure affect the gas sorption and diffusion processes in membranes. Based on this fact and taking into account the good gas transport properties of polyimide membranes, in earlier works [4–6] we proceeded to the study of gas transport in membranes prepared from norbornene monomers containing dicarboximide side groups with adamantyl, cyclohexyl and cyclopentyl moieties. In general, membranes prepared from these modified polynorbornenes have rather good permselectivity though low permeability attributed to strong interactions arising from the high polarity of the dicarboximide groups that reduces the free volume and local chain dynamics. It is worth noting that anchoring bulky side groups, such as the adamantyl moiety, to the dicarboximide groups to increase the free volume does not sufficiently increase the permeability of the membranes [4].

To improve the permeability of membranes based on polynorbornenes functionalized with substituted dicarboximide moieties

* Corresponding authors. Tel.: +52 5556224586; fax: +52 5556161201.
E-mail addresses: tma@servidor.unam.mx (M.A. Tlenkopatchev), mar@ictp.csic.es (M. López-González).

0376-7388/$ – see front matter © 2010 Elsevier B.V. All rights reserved.
doi:10.1016/j.memsci.2010.06.007

would require decreasing the favorable intermolecular interactions between molecular chains a goal that in principle can be accomplished by introducing fluorine atoms in either the main chain or in the substituted dicarboximide group moieties. Actually, the high electronegativity of fluorine severely reduces the polarizability of the atom in the C–F bond and as a result the formation of non-permanent or flitting dipoles which are the basis of the London dispersion forces [7]. As a result fluorocarbon moieties have very weak intermolecular attractive forces, thus increasing the free volume. In this regard, membranes prepared from poly[5,5-difluoro-6,6-bis(trifluoromethyl)norbornene] (PFMNB) and poly[5,5,6-trifluoro-6-(heptafluoropropoxy)norbornene] (POFPNB) [8] have permeability coefficients much higher than the membranes of non-substituted polynorbernene and even membranes prepared from polynorbornene containing alkyl moieties in their structures [1]. Preliminary studies carried out recently in poly(*N*-4-trifluoromethylphenyl-*exo*-*endo*-norbornene-5,6-dicarboximide) (TFMPNDI) and poly(*N*-3,5-bis(trifluoromethyl) phenyl-7-oxanorbornene-5,6-dicarboximide) (B3FMPONDI) showed a substantial increase of the permeability of the membranes with the fluorine content at expense of only a slight decrease in permselectivity [9]. Moreover, sorption studies carried out on polynorbornene membranes functionalized with substituted dicarboximide containing fluorinated moieties showed a significant increase in gas solubility [10]. Pursuing in this line of research and in order to get a deeper insight into the influence of the sp^3 and sp^2 hybridization of the carbon bonded to the fluorine bond on the sorption and diffusive steps of gas transport in membranes based on polynorbornene functionalized with dicarboximide side groups, we proceeded in this work to the synthesis of functionalized polynorbornenes in which the hydrogen of the imide group is replaced either by 3,5-bis(trifluoromethyl) or by perfluorinated phenyl moieties, specifically poly(*N*-3,5-bis(trifluoromethyl)phenyl-*exo*-*endo*-norbornene-5,6-dicarboximide) (PB3FMPNDI) and poly(*N*-pentafluorophenyl-*exo*-*endo*-norbornene-5,6-dicarboximide) (P5FPNDI). Membranes were cast from solutions of these polymers and the parameters associated with the sorption and diffusive steps of different gases in the membranes were compared with those reported earlier [4] for poly(*N*-phenyl-*exo*-*endo*-norbornene-5,6-dicarboximide) (PPNDI). These studies were extended to membranes obtained from poly(*exo*-*N*-pentafluorophenyl-7-oxanorbornene-5,6-dicarboximide) (P5FPONDI) with the aim of analyzing the effect of the increase of the polarity of the main chain on gas transport. The effect of increasing the dilution of the fluorocarbon moieties in the modified polynorbornenes was also examined in membranes cast from solutions of the random copolymer (50/50 mol) of *N*-pentafluorophenyl-*exo*-*endo*-norbornene-5,6-dicarboximide and *N*-phenyl-*exo*-*endo*-norbornene-5,6-dicarboximide) (P5FPNDI/PPNDI). The structures of the polymers used in this work are shown in Fig. 1. In some cases, sorption experiments of highly condensable gases accompanied the permeation experiments to study the effect of slight differences in structure on the dual-mode model parameters that describe gas transport of condensable gases in the membranes.

2. Experimental

2.1. Materials

Exo(90%)–*endo*(10%) mixture of norbornene-5,6-dicarboxylic anhydride (NDA) was obtained via Diels–Alder condensation of

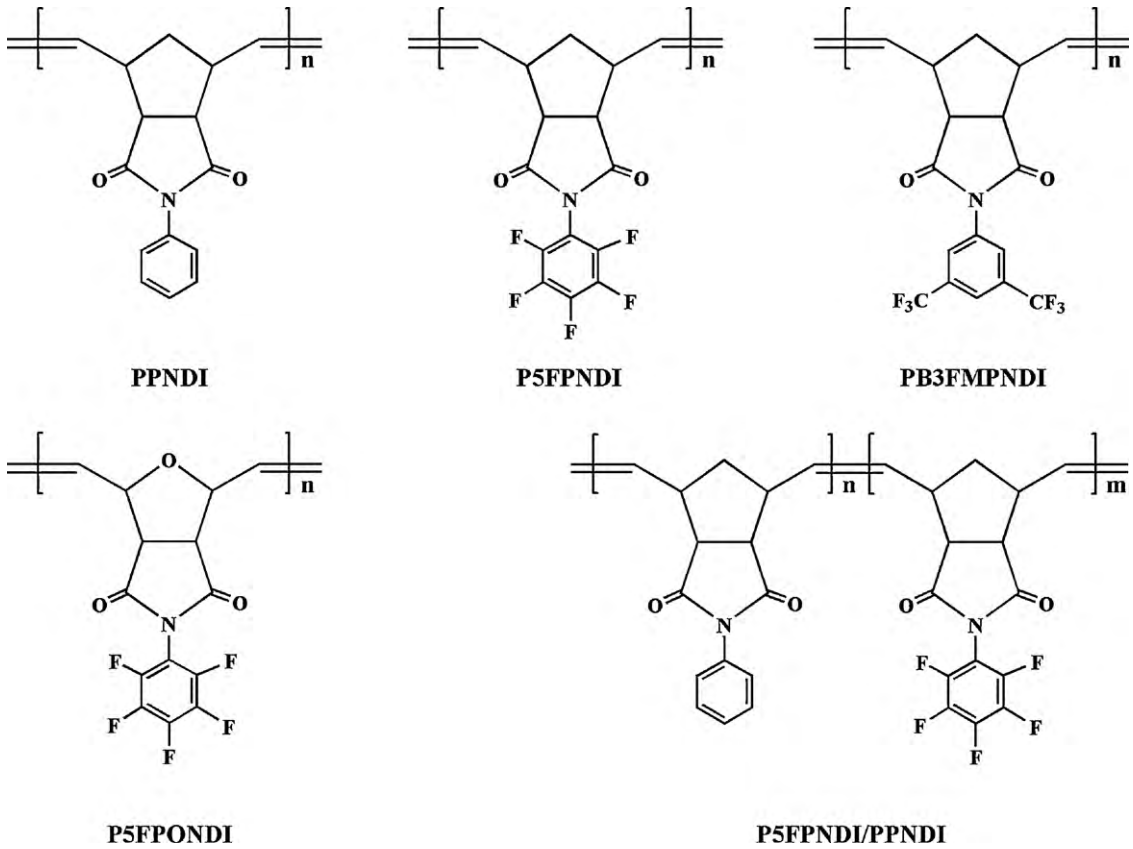

Fig. 1. Schemes of the repeat units of poly(*N*-phenyl-*exo*-*endo*-norbornene-5,6-dicarboximide) (PPNDI), poly(*N*-pentafluorophenyl-*exo*-*endo*-norbornene-5,6-dicarboximide) (P5FPNDI), poly(*N*-3,5-bis(trifluoromethyl)phenyl-*exo*-*endo*-norbornene-5,6-dicarboximide) (PB3FMPNDI), poly(*exo*-*N*-pentafluorophenyl-7-oxanorbornene-5,6-dicarboximide) (P5FPONDI) and random copolymer (50/50 M) P5FPNDI/PPNDI.

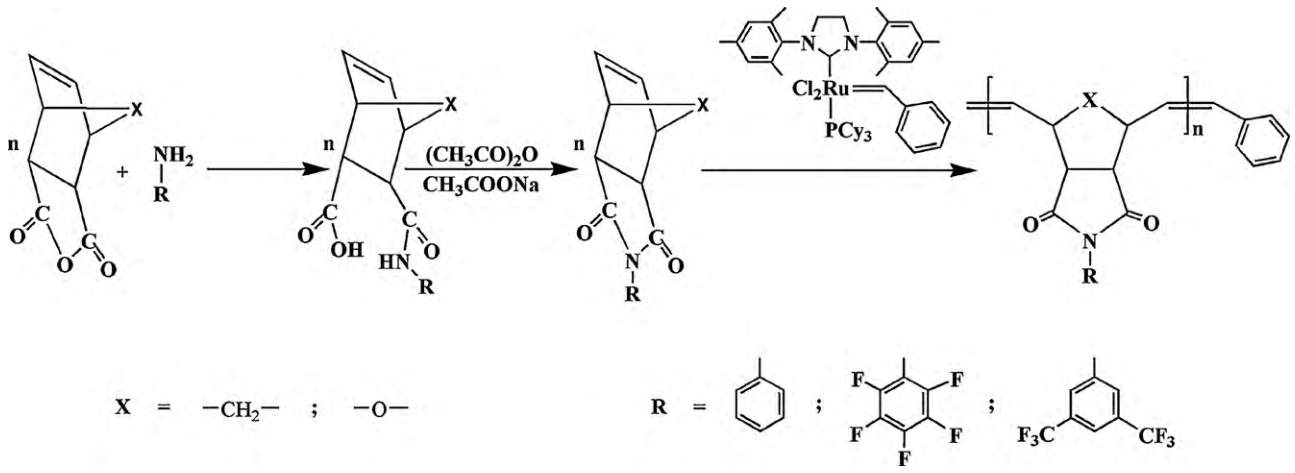

Fig. 2. Route of synthesis of monomers and further polymerization.

cyclopentadiene and maleic anhydride. *Exo*-7-oxanorbornene-5,6-dicarboxylic anhydride (ONDA), 3,5-bis(trifluoromethyl) aniline, 2,3,4,5,6-pentafluoroaniline and the catalyst tricyclohexylphosphine [1,3-bis(2,4,6-trimethylphenyl)-4,5-dihydroimidazol-2-ylidene][benzylidene] ruthenium dichloride (Aldrich Chemical Co.) were used as received. Other chemicals such as 1,2-dichloroethane, dichloromethane and toluene were dried over anhydrous calcium chloride and distilled over CaH_2.

2.2. Monomers synthesis

The route of synthesis of the monomers is shown in Fig. 2. Monomers were prepared in a similar way according to the methodology described previously [4]. Briefly, by reaction of NDA and ONDA with 2,3,4,5,6-pentafluoroaniline two amic acids are obtained which further treated with anhydrous sodium acetate/acetic anhydride produce, respectively, the new monomers *exo*-*N*-pentafluorophenyl-7-oxanorbornene-5,6-dicarboximide (5FPONDI) and *N*-pentafluorophenyl-*exo*-*endo*-norbornene-5,6-dicarboximide (5FPNDI) (see Fig. 2). In the same way *N*-3,5-bis(trifluoromethyl)phenyl-*exo*-*endo*-norbornene-5,6-dicarboximide (B3FMPNDI) was obtained. As an example, the details of the synthesis and characterization of *N*-pentafluorophenyl-*exo*-*endo*-norbornene-5,6-dicarboximide is given below: 5.58 g (30.5 mmol) of 2,3,4,5,6-pentafluoroaniline in 20 mL of dichloromethane were added to a stirred solution of NDA (5.0 g, 30.5 mmol) dissolved in 40 mL of dichloromethane. After 3 h at reflux, the reaction medium was cooled at room temperature and a precipitate was filtered and dried to give 10.3 g (29.7 mmol) of amic acid. A mixture of amic acid (10.3 g, 29.7 mmol), anhydrous sodium acetate (2.50 g, 30.47 mmol) and acetic anhydride were heated at 80 °C for 24 h. After cooling, the mixture was washed with dilute HCl and extracted into ether. The ether layer was washed with dilute HCl, saturated $NaHCO_3$ and H_2O. Solvent was evaporated and pure monomer 5FPNDI was obtained after twice recrystallization from hexane and dried in a vacuum oven at 50 °C overnight: yield = 75%; mp = 112–113 °C; ^{1}H NMR (300 MHz, $CDCl_3$), δ (ppm) = 6.36 (1H, s), 6.25 (1H, s), 3.53 (1H, s), 3.42 (1H, s), 2.96 (2H, s), 1.70–1.54 (2H, m); ^{13}C NMR (75 MHZ, $CDCl_3$): δ (ppm) = 174.7 (C=O), 147.8–139.6 (C–F), 137.8 (C=C), 134.4 (C=C), 107.1 (C–N), 52.1, 48.4, 45.8, 45.6, 42.9; ^{19}F NMR (300 MHz, $CDCl_3$, ref. TFA [−77 ppm]): δ (ppm) = −142.2, −142.4, −150.1, −150.6, −160.1, −160.4; FT-IR (KBr, cm^{-1}): 3076, 2949 (C–H asym str), 2880 (C–H sym str), 1782 (C=O), 1724, 1644 (C=C str), 1519, 1356, 1299 (C–F), 1172, 1157, 984, 793. Details of the synthesis and characterization of the other monomers are given in Supporting Information.

2.3. Polymerization

Polymerization of the monomers was carried out by ring opening metathesis polymerization (ROMP), at room temperature, in glass vials under nitrogen atmosphere. The polymerization was terminated by adding ethyl vinyl ether to the reaction medium which was further poured into methanol, solubilized with chloroform containing a few drops of 1 N HCl and precipitated again into methanol. The product was dried in a vacuum oven at 40 °C to constant weight. As an example, poly(*exo*-*N*-pentafluorophenyl-7-oxanorbornene-5,6-dicarboximide) was obtained by introducing 1.0 g of *exo*-*N*-pentafluorophenyl-7-oxanorbornene-5,6-dicarboximide (3.02 mmol) and 2.5×10^{-3} g (0.0030 mmol) of catalyst in a vial under nitrogen atmosphere. The reaction was carried out at 45 °C and stirred in 3.0 mL of 1,2-dichloroethane for 2 h (see Fig. 2). The polymer was separated using the protocol indicated above. The polymer was soluble in chloroform, toluene and 1,2-dichloroethane. ^{1}H NMR (300 MHz, $CDCl_3$): δ (ppm) = 6.10 (2H, s, *trans*), 5.86 (2H, s, *cis*), 5.0 (2H, s), 4.62 (2H, s), 3.55 (2H, s); ^{13}C NMR (75 MHz, $CDCl_3$): δ (ppm) = 172.2, 146.0, 140.5, 135.4, 130.6, 126.9, 106, 80.9, 53.8, 53.0; ^{19}F NMR (300 MHz, $CDCl_3$, ref. TFA [−77 ppm]): δ (ppm) = −142.5, −149.7, −159.7; FT-IR: 3088 (C=C–H asym str), 1790 (C=O), 1724 (C=O), 1652 (C=C str), 1479 (C–H), 1336 (C–F), 1289 (C=C–H), 1179 (C–O–C asym str), 848 cm^{-1} (C–C str). See Supporting Information for the details of the synthesis and characterization of the rest of polymers.

2.4. Glass transition temperatures and molecular weights

Glass transition temperatures, T_g, were determined in a DSC-7 Perkin Elmer Inc., at scanning rate of 10 °C/min under nitrogen atmosphere. The samples were encapsulated in standard aluminum DSC pans. Each sample was run twice on the temperature range between 30 °C and 300 °C. Molecular weights and molecular weight distributions were determined with reference to polystyrene standards on a Waters 2695 ALLIANCE GPC at 35 °C in tetrahydrofuran using a universal column and a flow rate of 0.5 mL min^{-1}. The results for the number average molecular weight M_n, molecular weight heterodispersity index M_w/M_n and glass transition temperature T_g of the polymers are collected in Table 1.

Table 1
Number average molecular weight M_n, heterodispersity index M_w/M_n, glass transition temperature T_g, density ρ, free volume v_f and fractional free volume *FFV* of poly(*N*-phenyl-*exo*-*endo*-norbornene-5,6-dicarboximide) (PPNDI), poly(*N*-pentafluorophenyl-*exo*-*endo*-norbornene-5,6-dicarboximide) (P5FPNDI), poly(*N*-3,5-bis(trifluoromethyl)phenyl-*exo*-*endo*-norbornene-5,6-dicarboximide) (PB3FMPNDI), poly(*exo*-*N*-pentafluorophenyl-7-oxanorbornene-5,6-dicarboximide) (P5FPONDI) and random copolymer (50/50 M) P5FPNDI/PPNDI.

Membrane	$M_n \times 10^5$, g/mol	M_w/M_n	T_g, °C	ρ, g/cm^3	v_f, cm^3/g	*FFV*
PPNDI	2.10	1.30	222	1.170	0.160	0.187
P5FPNDI	3.07	1.62	171	1.457	0.136	0.199
PB3FMPNDI	3.27	1.22	168	1.414	0.141	0.199
P5FPONDI	2.97	1.44	187	1.557	0.114	0.178
P5FPNDI/PPNDI	3.10	1.67	205	1.376	0.116	0.159

2.5. Membranes preparation, permeation and sorption experiments

Membranes were cast from polymer solutions in chloroform and dimethylformamide at room temperature. The density of the membranes was measured at room temperature by the flotation method using ethanol as liquid. The values of the density are shown in Table 1.

Permeation experiments were carried out in a cell made of two semi-cells separated by the membrane. After making vacuum in the two semi-cells, gas at a given pressure is introduced into the high pressure or upstream semi-cell, which is coupled to a Gometrics pressure transducer. The gas flowing across the membrane to the low pressure or downstream semi-cell is monitored as a function of time with a MKS 628/B pressure transducer via a PC. Permeation cell is kept inside a water thermostat at the temperature of interest. If the volume V of the downstream semi-cell is given in cm^3, the area A of the exposure membrane in cm^2, its thickness l in cm and the pressure in cm Hg, the permeability coefficient P of the gases in the membranes in barrer [1 barrer = 10^{10} cm^3 (STP) cm/(cm^2 s cm Hg)], is given by

$$P = 3.59\frac{Vl}{p_0 AT}\lim_{t\to 0}\left(\frac{dp}{dt}\right) \quad (1)$$

where T is the absolute temperature and p_0 and p are, respectively, the upstream and downstream gas pressures. The p *vs* t isotherms present a transitory followed by a straight line ($t \to \infty$) corresponding to steady state conditions. The intersection of the straight line with the abscissa axis of the plot is the time-lag θ, related to the apparent gas diffusion coefficient by [11].

$$D = \frac{l^2}{6\theta} \quad (2)$$

The diffusion coefficient is currently given in D in cm^2/s units. The apparent solubility coefficient, S, is given by

$$S = \frac{P}{D}$$

The usual units of S are cm^3 (STP)/(cm^3 cm Hg).

Sorption experiments were performed in a sorption cell separated from a reservoir containing the gas at the desired pressure by means of a valve [12]. The experimental device is immersed in a water thermostat bath. Circular films, about 0.1 mm thick and separated by metallic grids to facilitate gas sorption, are introduced into the sorption cell which is coupled to a Ruska pressure transducer. Keeping open the valve separating the reservoir and the sorption cell vacuum is made in both compartments and then the valve is closed. Gas at the desired pressure is introduced into the reservoir and the gas is allowed to flow into the permeation cell by suddenly open and close the valve. The diminution of pressure in the sorption cell with time by effect of the sorption process is monitored with the pressure transducer via a PC. Once steady state condition is accomplished, gas at higher pressure flows from the reservoir to the sorption cell by suddenly opening a closing the valve and the evolution of the pressure is monitored as in the first step and so on. The concentration of gas at the step i is given by

$$c_i = \frac{22,414\rho V}{mRT}\left(\frac{p_{i1}}{z_{i1}} - \frac{p_{i2}}{z_{i2}}\right) \quad (3)$$

where m and ρ are, respectively, the mass and density of the membrane in the sorption cell, R and T are, respectively, the gas constant and the absolute temperature at which the experiment is performed, p_{i1} and p_{i2} are, respectively, the pressure of the gas in the sorption cell at $t \to 0$ and $t \to \infty$ and z_{i1} and z_{i2} are the compressibility coefficients of the gases at pressures p_{i1} and p_{i2}. The concentration of gas in the membranes is usually given in cm^3 (STP)/cm^3.

3. Results

Values of the permeability, diffusion and apparent solubility coefficients for several gases in the membranes P5FPNDI, PB3FMPNDI, P5FPONDI and P5FPNDI/PPNDI, at 30 °C, are shown in Table 2. In the same table and for comparative purposes the values of these coefficients for the non-fluorinated polymer, poly(*N*-phenyl-*exo*-*endo*-norbornene-5,6-dicarboximide) (PPNDI), reported earlier [4], are also shown. In general, the permeability coefficients of the gases in the membranes follow the trends $P(H_2) > P(CO_2) > P(O_2) > P(C_2H_4) > P(CH_4) \geq P(N_2) > P(C_3H_6) > P(C_2H_6)$ that differ from those for the diffusion coefficient which decrease in the order $D(H_2) > D(O_2) > D(N_2) > D(CO_2) > D(CH_4) > D(C_2H_4) > D(C_2H_6) > D(C_3H_6)$. Obviously CO_2 and the most condensable hydrocarbon gases exhibit the larger apparent solubility coefficients in such a way that $S(C_3H_6) > S(CO_2) > S(C_2H_4) > S(C_2H_6) > S(CH_4) > S(O_2) > S(N_2) > S(H_2)$.

As usual, the temperature dependence of the permeability, diffusion and apparent solubility coefficients follows Arrhenius behavior as the illustrative plots of the natural logarithm of these parameters against the reciprocal of temperature for oxygen, methane and carbon dioxide in the P5FPNDI membrane show (see Fig. 3). The activation energies associated with the permeability, diffusive and sorption steps obtained from the slopes of the corresponding Arrhenius plots are collected in Table 3.

The sorption characteristics of the most condensable gases CO_2 and C_3H_6 in the P5FPNDI membrane were studied and illustrative results of the dependence of the concentration on pressure, at two temperatures, are shown in Fig. 4. The results expressed in terms of the solubility coefficient, presented in Fig. 5, show that the absolute solubility coefficient sharply decreases at low pressures and then moderately reaching a nearly constant value at pressures in the vicinity of 900 cm Hg. As usual in glassy membranes, the solubility coefficient obeys the dual-mode model that assumes that the membrane is made up of a continuous phase in which microcavities of Langmuir sites accounting for the excess volume are dispersed. In the continuous phase, the solubility obeys to Henry's law whereas in the Langmuir sites adsorption processes govern the solubility. Accordingly, the dependence of the solubility coefficient

Table 2
Values of the permeability, diffusion and apparent solubility coefficient of different gases, at 30 °C, in membranes of poly(*N*-phenyl-*exo*-*endo*-norbornene-5,6-dicarboximide) (PPNDI), poly(*N*-pentafluorophenyl-*exo*-*endo*-norbornene-5,6-dicarboximide) (P5FPNDI), poly(*N*-3,5-bis(trifluoromethyl)phenyl-*exo*-*endo*-norbornene-5,6-dicarboximide) (PB3FMPNDI), poly(*exo*-*N*-pentafluorophenyl-7-oxanorbornene-5,6-dicarboximide) (P5FPONDI) and random copolymer (50/50 M) P5FPNDI/PPNDI.

Membrane	Gas	*P*, barrer	$D \times 10^8$, cm²/s	$S \times 10^3$, cm³ (STP)/(cm³ cm Hg)
PPNDI	H_2	11.0	132.0	0.83
	N_2	0.31	2.23	1.39
	O_2	1.44	6.30	2.29
	CO_2	11.44	1.81	63.20
	CH_4	0.54	0.72	7.50
	C_2H_6	0.09	0.40	2.25
	C_2H_4	0.58	0.30	19.33
	C_3H_6	–	–	–
P5FPNDI	H_2	38.50	112.14	3.43
	N_2	1.55	2.51	6.15
	O_2	6.08	7.64	7.96
	CO_2	25.17	1.50	170.64
	CH_4	1.37	0.64	21.37
	C_2H_6	0.70	0.05	141.99
	C_2H_4	3.06	0.21	147.30
	C_3H_6	1.24	0.05	229.53
PB3FMPNDI	H_2	57.41	351.54	1.63
	N_2	4.20	8.27	5.08
	O_2	13.53	18.66	7.24
	CO_2	67.26	4.81	139.71
	CH_4	4.28	3.29	13.03
	C_2H_6	2.62	0.32	82.72
	C_2H_4	6.91	0.74	93.02
	C_3H_6	3.79	0.16	239.59
P5FPNDI/PPNDI	H_2	19.55	106.68	1.83
	N_2	0.59	1.15	5.16
	O_2	2.66	3.78	7.02
	CO_2	16.51	0.91	180.6
	CH_4	0.64	0.31	20.61
	C_2H_6	0.35	0.03	140.93
	C_2H_4	1.32	0.08	163.76
	C_3H_6	0.70	0.01	517.66
P5FPONDI	H_2	22.92	200.21	1.14
	N_2	1.08	3.06	3.54
	O_2	3.55	7.47	4.75
	CO_2	16.30	1.47	110.62
	CH_4	1.13	1.00	11.37
	C_2H_6	0.54	0.09	58.03
	C_2H_4	1.69	0.23	73.07
	C_3H_6	0.67	0.04	167.21

on pressure is given by [12–14]

$$S = k_D + \frac{C'_H b}{1 + bp} \tag{4}$$

where k_D is the Henry solubility constant, C'_H is the concentration of gas in Langmuir sites and b is a parameter accounting for the affinity gas-membrane. Values of k_D, C'_H and b for CO_2 and C_3H_6 at several temperatures are shown in Table 4. In the same table and for comparative purposes the values at 30 °C of these parameters in the membrane PB3FMPNDI are also shown. The variation of the dual-mode model solubility parameters with the reciprocal of temperature for CO_2 and C_3H_6, shown in Fig. 6, suggests that both k_D and b are strongly dependent on temperature whereas C'_H is comparatively much less sensitive to temperature. The activation energies corresponding to k_D, C'_H and b are collected in Table 5.

The variation of the permeability coefficient and the diffusion coefficients of CO_2 and C_3H_6 in the membranes P5FPNDI and PB3FMPNDI with pressure are shown in Fig. 7. As for the solubility coefficient, a substantial decrease in the values of the permeability coefficient of CO_2 with increasing pressure is observed, at low pressures, reaching a minimum at 10 bar, and then P increases with increasing pressure. The pressure dependence of the permeability coefficient of C_3H_6 is similar, though in this case the minimum of the value of P is reached at lower pressure, about 4 bar. The drop of P with p in the range of pressures below the minimum of the sorption curve is described by the partial immobilization dual-mode model given by [14,15]

$$P = k_D D_D + \frac{C'_H b D_H}{1 + bp} = k_D D \left[1 + \frac{FK}{1 + bp}\right] \tag{5}$$

where D_D and D_H are, respectively, the diffusion coefficients in the continuous phase and Langmuir sites, $K = bC'_H/k_D$ and $F = D_H/D_D$. Using for b in Eq. (5) the values obtained for this parameter in the sorption results, the plots P *vs* $1/(1 + bp)$ give reasonable straight lines whose slopes and ordinates in the origin yield, respec-

Table 3
Activation energies associated with the permeability (E_P) and diffusion (E_D) coefficients and apparent sorption heat (ΔH_s) for different gases in poly(*N*-pentafluorophenyl-*exo*-*endo*-norbornene-5,6-dicarboximide) (P5FPNDI), at 1 bar.

Gas	E_P, kcal/mol	E_D, kcal/mol	ΔH_s, kcal/mol
H_2	2.76	1.42	1.34
N_2	3.10	7.10	−3.99
O_2	2.22	5.77	−3.55
CO_2	0.30	7.15	−6.85
CH_4	3.81	8.51	−4.70
C_2H_6	3.63	9.25	−5.62
C_2H_4	2.44	8.55	−6.11
C_3H_6	2.36	9.21	−6.85

Table 4
Values at 30 °C of the Henry's solubility constant, k_D, gas concentration in Langmuir sites, C'_H, affinity parameter, b, enthalpic interaction parameter, χ, gas diffusion coefficients in the continuous phase, D_D, and Langmuir sites, D_H, of P5FPNDI and PB3FMPNDI membranes.

Gas	T, (°C)	$10^3 \times k_D$, cm^3 (STP)/cm^3 cm Hg	C'_H, cm^3 (STP)/cm^3	$10^3 \times b$, (cm Hg)$^{-1}$	χ	$10^8 \times D_D$, cm^2/s	$10^8 \times D_H$, cm^2/s
P5FPNDI membrane							
CO_2	20	46.03	14.97	22.85	+0.37	–	–
	30	30.84	14.34	9.85	+0.54	6.08	0.95
	40	26.70	13.59	7.38	+0.47	–	–
	50	22.25	12.79	5.15	+0.44	–	–
C_3H_6	30	66.97	10.71	83.66	+1.26	0.15	0.03
	40	64.29	9.03	81.88	+1.13	–	–
	50	34.11	12.11	30.28	+1.81	–	–
	60	28.76	9.69	32.83	+1.61	–	–
PB3FMPNDI membrane							
CO_2[a]	30	18.8	10.2	6.9	+1.04	27.45	3.16
C_3H_6[a]	30	37.1	13.4	24.4	+1.81	0.63	0.08

[a] Taken from Ref. [10].

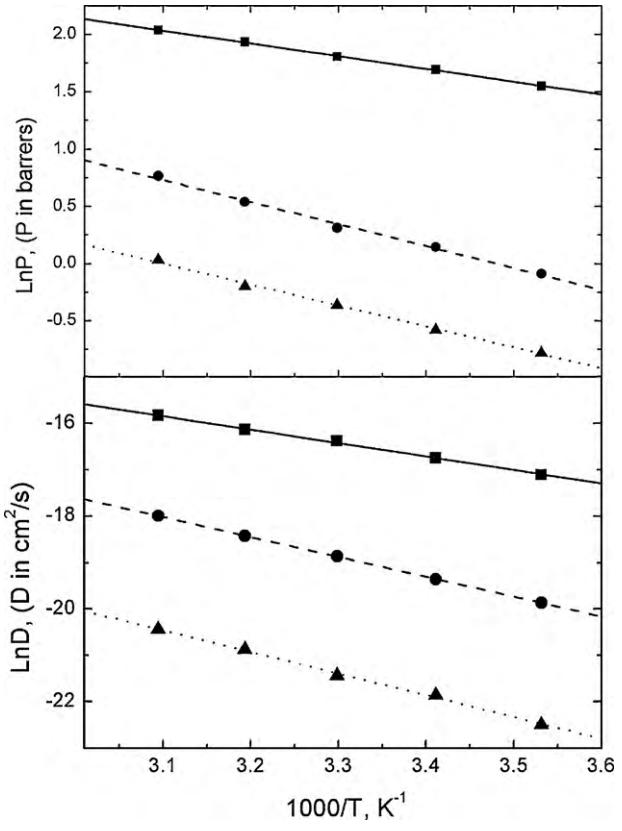

Fig. 3. Arrhenius plots for the permeability and diffusion coefficients of oxygen (squares), methane (triangles) and propylene (circles) in poly(*N*-pentafluorophenyl-*exo-endo*-norbornene-5,6-dicarboximide) (P5FPNDI) membrane.

tively, $C'_H bD_H$ and $K_D D_D$ (see Fig. 8). These results combined with those found for k_D, C'_H and b in the sorption experiments of CO_2 at 30 °C yield for $10^8 \times D_D$ and $10^8 \times D_H$ the values of 6.08 and 0.95 cm^2/s for the P5FPNDI membrane and 27.45 and 3.16 cm^2/s for the PB3FMPNDI membrane.

Table 5
Activation energies in kcal mol^{-1} associated with the solubility constant at 76 cm Hg, E_s, Henry's constant, E_D, gas concentration at Langmuir sites, $E_{C'_H}$, and the affinity gas-membrane parameter, E_b for the P5FPNDI membrane.

Gas	E_S, kcal/mol	E_D, kcal/mol	$E_{C'_H}$, kcal/mol	E_b, kcal/mol
CO_2	−6.5	−4.42	−0.99	−9.06
C_3H_6	−3.02	−6.37	−0.01	−7.67

4. Discussion

The fluorinated membranes presumably have significant surface fluorine content compared to the theoretical bulky fluorine content owing to the low surface energy of fluorinated moieties [16] which provide a thermodynamic driving force for the self-assembly of these moieties at the surface air–polymer interface. Moreover, segregation may occur of structural units containing phenyl groups from those with pentafluorophenyl moieties in the copolymer giving rise to the formation of two types of nanosize domains in the P5FPNDI/PPNDI membrane.

The presence of fluorine atoms in the substituted imide side groups increases the permeability of the polynorbornene membranes as reveals the fact that the permeability coefficients of the gases in the P5FPNDI membrane are three to four times larger than those in the non-fluorinated PPNDI membrane. However, the increase in permeability in the P5FPNDI membrane does not arise from diffusive process but from the gas sorption step. Thus the apparent solubility coefficient of the light and condensable gases in the membrane P5FPNDI is, respectively, about 5 and 10–20 times higher than in the PPNDI. Moreover, the increase in the degree of hybridization of the carbon atom in the C–F bonds apparently causes a diminution of the solubility of the gases in fluorinated membranes. The sorption results for CO_2 and C_3H_6 in P5FPNDI and PB3FMPNDI membranes, collected in

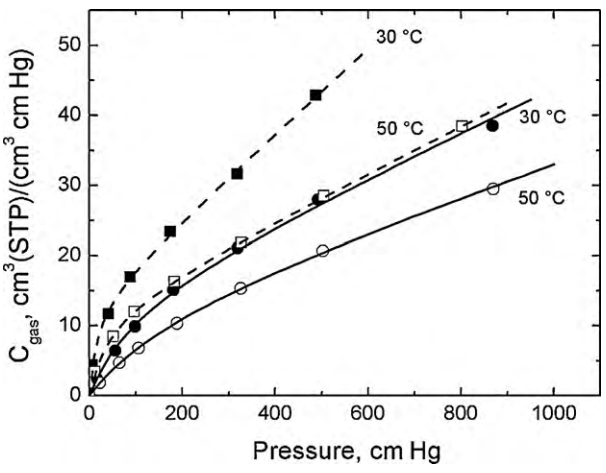

Fig. 4. Illustrative plots showing the variation of the concentration of propylene (squares) and carbon dioxide (circles) with pressure at 30 °C (filled symbols) and 50 °C (open symbols) in poly(*N*-pentafluorophenyl-*exo-endo*-norbornene-5,6-dicarboximide) (P5FPNDI) membrane.

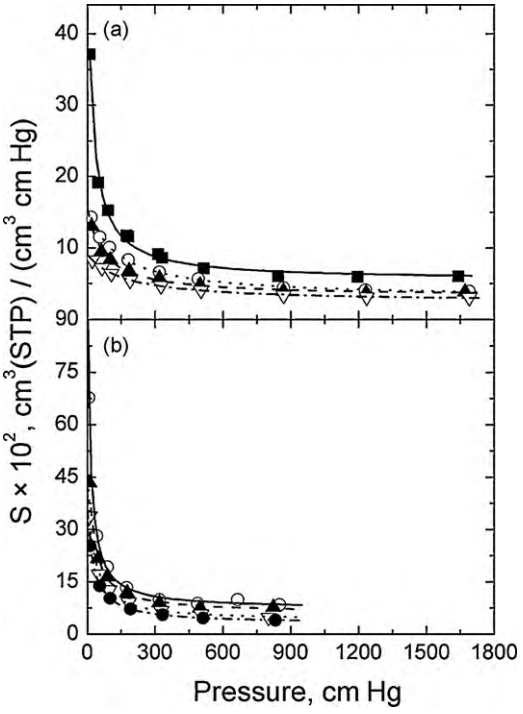

Fig. 5. Variation of the solubility coefficient of carbon dioxide (a, top) and propylene (b, bottom) with pressure in P5FPNDI membranes at several temperatures: (■) 20 °C, (○) 30 °C, (▲) 40 °C, (▽) 50 °C and (●) 60 °C.

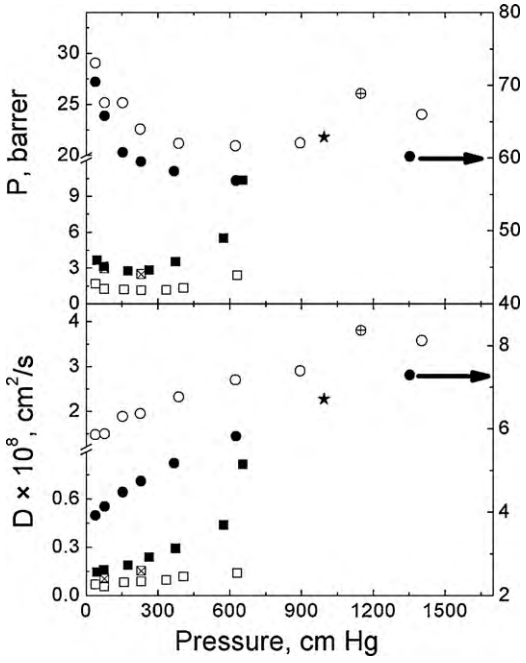

Fig. 7. Variation of the permeability coefficients (top) and the diffusion coefficient (bottom) of CO_2 (circles) and C_3H_6 (squares), at 30 °C in P5FPNDI (open symbols) and PB3FMPNDI (filled symbols). The symbols ⋆ (CO_2 in PB3FMPNDI), ⊕ (CO_2 in P5FPNDI) and ⊠ (C_3H_6 in P5FPNDI) correspond to measurements immediately made after the experiment performed at the highest pressure used in the corresponding isotherms.

Table 4, show that the variation of the solubility of the gases with variations in structure mainly occurs in the Henry's solubility constant. For example, the values of $k_D \times 10^3$ for CO_2, in the P5FPNDI and PB3FMPNDI membranes are, at 30 °C, 30.8 and 18.8 cm^3 (STP)/(cm^3 cm Hg), respectively. The results for C_3H_6 are, 67.0×10^{-3} and 37.1×10^{-3} cm^3 (STP)/(cm^3 cm Hg), respectively. The increase in solubility in membranes with imide side groups containing fluorinated moieties is in consonance with the unique solvent properties attributed to fluorinated polymers and low molecular weight fluorine-containing organic compounds. This behavior may be the result of the specially low surface tension and cohesive energy density of fluorinated polymers [17–19]. On the other hand, the replacement of the CH_2 bond by an oxygen atom in the norbornene unit decreases the solubility of the gases in the membranes as the comparison of the apparent solubilities of the gases in P5FPNDI and P5FPONDI membranes show. The permeability performance of membranes prepared from modified polynorbornenes with the bulky adamantyl moiety attached to the dicarboximide, i.e. poly(*N*-adamantyl-norbornene-5,6-dicarboximide) [4], is significantly lower than that of the P5FPNDI and PB3FMPNDI membranes leading to conclude that the possible disruption of chain packaging by effect of the bulky adamantyl group is not so effective in improving gas transport as the presence of C–F bonds in the molecular chains of the latter membranes. On the other hand it is worth noting that the probable existence of two kinds of nanosize domains corresponding to phenyl and pentafluorophenyl moieties in the P5FPNDI/PPNDI membrane does not increase the permeability, but reduces it. In

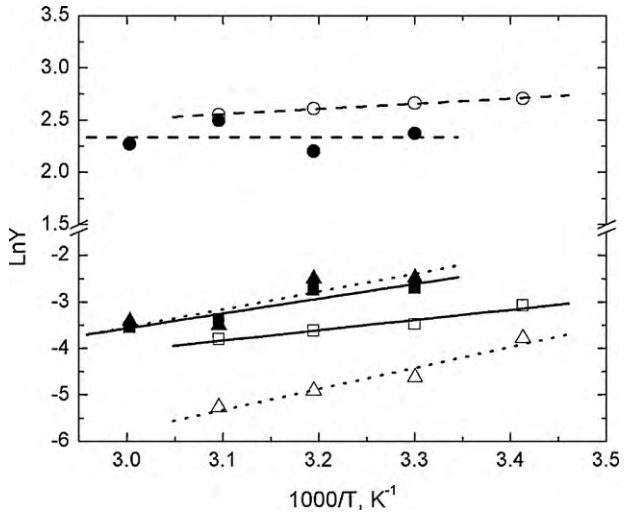

Fig. 6. Arrhenius plots for the dual-mode model parameters in P5FPNDI membrane: k_D (squares), C'_H (circles) and b (triangles). Open and filled symbols correspond, respectively, to carbon dioxide and propylene.

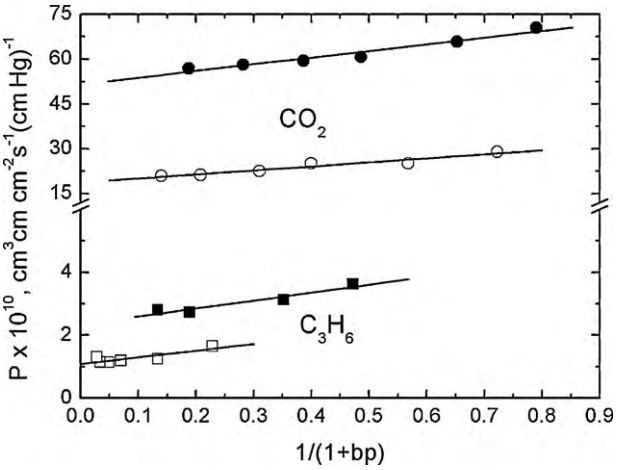

Fig. 8. Fitting of Eq. (5) to the permeability results, at 30 °C, for CO_2 (circles) and propylene (squares) in P5FPNDI (open symbols) and PB3FMPNDI (full symbols) membranes.

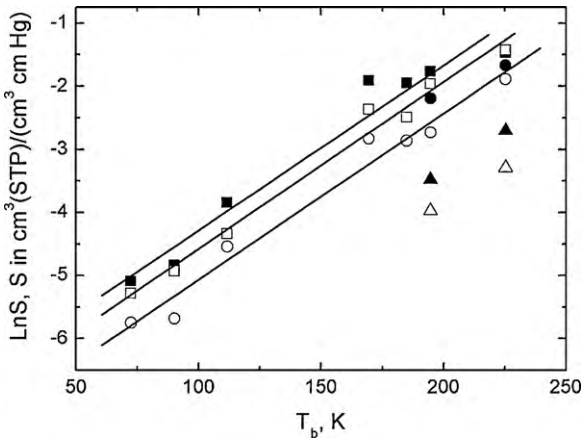

Fig. 9. Dependence of the apparent (squares) and absolute (circles) solubility coefficients, at 1 bar and 30 °C, on the boiling temperature of the gases in P5FPNDI (full symbols) and PB3FMPNDI (open symbols). Triangles correspond to the Henry's constant.

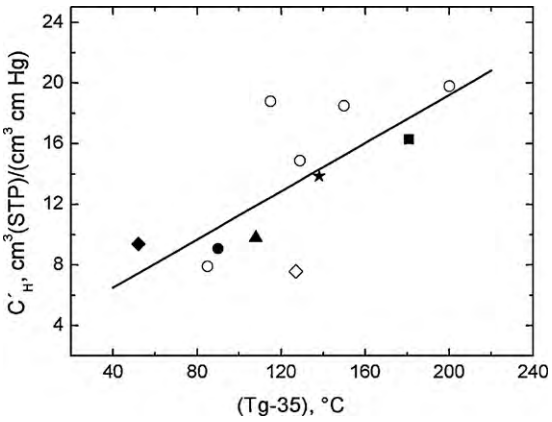

Fig. 10. Values of C'_H against $T_g - T$ for: (○) polycarbonates; (♦) copolyester; (▲) poly(ether ether ketone); (■) poly(ether-imide); (●) copolynorbornene dicarboximide; (◊) fluorinated polynorbornene dicarboximide; (★) present work.

fact, the permeability coefficient of the gases in the membrane is below the average of the coefficients of the gases of interest in the P5FPNDI and PPNDI membranes.

The effect of temperature on the permeation and diffusive steps was studied in the P5FPNDI membrane. For all gases but hydrogen, the activation energy associated with the permeability coefficient of the gases is positive and $E_P - E_D < 0$ (see Table 3). Then with the exception of hydrogen the sorption step is an exothermic process that increases with gas condensability.

To rationalize the solubility of the gases in membranes it is convenient to interpret the results in terms of the expression obtained for the sorption process from the change in free energy arising from the mixture of the gas in the liquid state with the polymer chains. The pertinent expression for the gas solubility in the continuous phase of the membrane in the dual-mode model is given by [20,21]

$$k_D = \frac{22,414}{76\overline{V}} \exp\left[-(1+\chi) - \frac{\lambda_b}{RT_b}\left(1 - \frac{T_b}{T}\right)\right] \quad (6)$$

where $\overline{V}$ is the partial molar volume in cm^3/mol of the gas in the liquid state, T_b is the boiling temperature in K of the gas in the liquid state at 1 bar, λ_b is the latent heat of vaporization at T_b, χ is a dimensionless gas (in the liquid state)—polymer enthalpic parameter, R is the gas constant and T is the working temperature in K. The application of Eq. (6) to the results obtained for k_D of CO_2 and C_3H_6 in P5FPNDI membranes by the dual-mode model gives for χ the results shown in Table 4. For example, the values of χ for CO_2 and C_3H_6 in the P5FPNDI membrane, at 30 °C, are 0.54 and 1.26, respectively. In the PB3FMPNDI membrane, these values augment to 1.04 and 1.81 for CO_2 and C_3H_6, respectively. It seems that the strong quadripole moment of CO_2 favors interactions between this gas and the polar fluorinated moieties. According to Eq. (6), as T approaches T_b, i.e. the condensability of the gas increases, k_D undergoes a significant increase. Taking into account that the average of λ_b/RT_b for most gases is 9.21 ± 0.82 and considering that χ lies in the vicinity of the unit, a plot of $\ln(k_D\overline{V})$ *vs* T_b should give a reasonable straight line. As shown in Fig. 9, parallel straight lines fit the plot of the natural logarithms of the absolute and apparent values of the solubility coefficients *vs* T_b plots in concordance with Eq. (6). The same occurs with the values of $\ln k_D$ *vs* T_b but in this case the fitting straight lines lie below those corresponding to S. Notice that the slope of the plots is rather close to that predicted by Eq. (6) taking into account the assumptions indicated.

On the other hand, since an increase in the glass transition temperature also increases the excess volume of the glassy polymer at the working temperature, the gas concentration in the Langmuir sites should increase as T_g increases. Actually by assuming that C'_H is proportional to the excess in volume the value of this quantity can be estimated as [22,23]

$$C'_H = 22,414k'_H \frac{V^{excess}}{\overline{V}} = \frac{22,414k'_H}{\overline{V}}\left(\alpha_l - \alpha_g\right)\left(T_g - T\right) \quad (7)$$

where $\alpha_i = (1/V)(\partial V/\partial T)_p$, $i = l, g$, is the expansion coefficient. Since α_l lies in the range $(4\text{–}6) \times 10^{-4}\ K^{-1}$ and $\alpha_g \ll \alpha_l$, C'_H should be a linear function of T_g–T. Experimental values of C'_H for CO_2 in several polymers such as (○) polycarbonates [24,25]; (♦) copolyester [26]; (▲) poly(ether ether ketone) [27]; (■) poly(ether-imide) [27]; (●) copolynorbornene dicarboximide [5], plotted as a function of T_g–T in Fig. 10, are close to those predicted by Eq. (7). The value of C'_H in P5FPNDI (●) fits to Eq. (7), but it lies below that predicted by Eq. (7) in PB3FMPNDI (◊) [10].

The comparison of the transport processes of the membranes P5FPNDI and PB3FMPNDI shows that the permeability coefficient of the gases in the latter membrane is nearly two times the value of this quantity in the former. As the results of Table 2 reveal, the diffusive step and not the sorption process is responsible for this behavior suggesting that the bulky 3,5-bis(trifluoromethylphenyl) group hinders chains packaging increasing the free volume and hence gas diffusion. The schematic replacement of the methylene group in the norbornene moieties of P5FPNDI by an oxygen atom yields the P5FPONDI chains. An inspection of the permeation characteristics of membranes prepared from P5FPONDI shows an increase in the diffusion coefficient compensated by a reduction of solubility in such a way that the permeability coefficient of the gases in P5FPNDI and P5FPONDI membranes is rather similar. The dilution of pentafluorophenyl moieties in the chains reduces the diffusion coefficient of the membranes as the comparison of the results for P5FPNDI and P5FPNDI/PPNDI membranes shows.

The free volume promotes the diffusive process across membranes. According to the free volume theory, the diffusion of the gases in membranes is governed by the equation [28]

$$D = D_0 \ \exp(-\gamma v* / v_f) \quad (8)$$

where γ is a parameter close to the unit, and $v*$ and v_f are, respectively, the critical volume just large enough to allow the displacement of molecules and the free volume. The free volume, customarily calculated by the Bondi method [29], was estimated as $v_f = v - 1.3v_w$ where v and v_w are, respectively, the specific volume of the membrane and the van der Waals volume estimated using van Krevelen's data [30]. Then the fractional free volume can be calculated as $FFV = \rho v_f$ where ρ is the density of the membrane. The values obtained for the fractional free volume of the membranes are

given in Table 1. An analysis of the diffusion coefficients of the gases in terms of Eq. (8) shows a fairly good correlation between diffusion and free volume for some gases such as hydrogen, oxygen, nitrogen, carbon dioxide and methane (see Fig. 1 of Supporting Information) whereas for other gases both parameters are uncorrelated. The lack of correlation may be attributed to several drawbacks involved in the estimation of the van der Waals volumes of the norbornene ring and the substituted dicarboximide group. These volumes were approximated by building the ring and the dicarboximide group in a stepwise fashion from known components. This procedure may introduce error in the calculated values of the free volume because it is based on some questionable assumptions the most important being that the volume occupied by a particular atom does not depend on its environment or chemical state [24]. Moreover, there are situations in which membranes with similar fractional free volume exhibit different diffusivities. This issue was examined by Wang et al. [31] using simulation techniques finding that not only the free volume but also the distribution of cavities affects the diffusive process.

The diffusion coefficient of condensable gases, such as CO_2 and C_3H_6, determined by the time-lag method, increases as pressure increases. Moreover, the analysis of the permeation and sorption results in terms of the dual-mode model indicates that the ratio between the diffusion coefficient in the Langmuir sites and in the continuous phase for CO_2 and C_3H_6 is, respectively, 0.16 and 0.20 in the membrane P5FPNDI and 0.12 and 0.13, respectively, in the PB3FMPNDI membrane. The dependence of the average diffusion coefficient on pressure can be estimated from the variation of the permeability with pressure in the region where P decreases with p and the dual-mode model holds. Taking into account that the concentration of gas in the membrane is $C = C_D + C_H$ where $C_D = k_D p$ and $C_H = bC'_H p/(1 + bp)$, the partial immobilized model suggests that the average diffusion of gas in steady state conditions depends on concentration in such a way that Fick's first law can be written as

$$J = -D_D \left[\frac{1 + FK/(1+bp)^2}{1 + K/(1+bp)^2} \right] \frac{\partial C}{\partial x} = -D_{DM}(C) \frac{\partial C}{\partial x} \tag{9}$$

where

$$D_{DM}(C) = D_D \left[\frac{1 + FK/(1+bp)^2}{1 + K/(1+bp)^2} \right] \tag{10}$$

The evolution of the values of D_{DM} corresponding to CO_2 and C_3H_6 with concentration in the P5FPNDI and PB3FMPNDI membranes is shown in Figs. 11 and 12. In both cases the diffusion coefficient increases with concentration in the whole range of concentrations where the pressure dependence of the permeability coefficient is governed by the dual-mode model, i.e. the permeability coefficient decreases with decreasing pressure until a constant value is obtained ($p \to \infty$). However, the results of Fig. 7 show that P reaches a minimum at $p = 625$ and 627 cm Hg for CO_2 in P5FPNDI and PB3FMPNDI, respectively, and 226 and 175 cm Hg, respectively, for C_3H_6. At pressures above the minimum the permeability coefficient of the gases increases with increasing pressure. Owing to the fact that the solubility coefficient continuously decrease with increasing pressure until a constant value is obtained at $p \to \infty$, the increase of P with p at high pressures must be attributed to the diffusive step. In this case it is better to define an effective diffusion coefficient, D_{eff}, obtained directly from experimental results involving the concentration dependences of both the permeability coefficient and the concentration. In the configuration used, the pressure in the downstream chamber is negligible with regard to that of the upstream chamber and the gas flux across the mem-

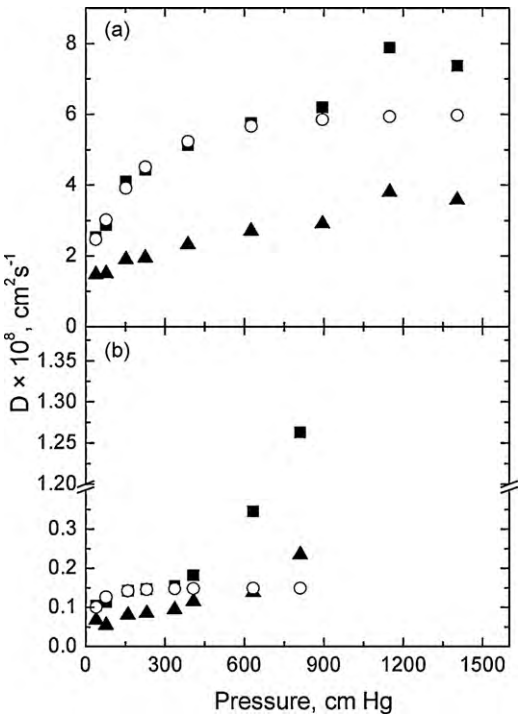

Fig. 11. Variation with pressure of the diffusion coefficients of CO_2 (a, top) and C_3H_6 (b, bottom) obtained by the time-lag method, D_θ (up-triangles), the dual-mode model, D_{DM} (circles), and permeation-sorption results, D_{eff} (squares), in the P5FPNDI membrane.

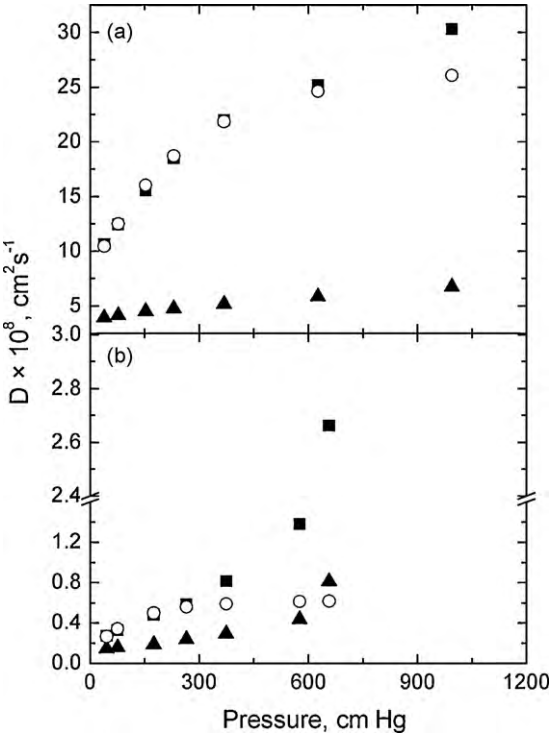

Fig. 12. Variation with pressure of the diffusion coefficients of CO_2 (a, top) and C_3H_6 (b, bottom) obtained by the time-lag method, D_θ (up-triangles), the dual-mode model, D_{DM} (circles), and permeation-sorption results, D_{eff} (squares), in the PB3FMPNDI membrane.

Table 6
Permselectivity coefficients for different pair of gases in the membranes, at 30 °C. Values between brackets correspond to the permeability coefficient of the less permeable gas of the pair of gases.

Sample	α_{O_2/N_2}	α_{CO_2/CH_4}	$\alpha_{C_2H_4/C_2H_6}$	α_{H_2/CH_4}	α_{H_2/C_2H_6}	α_{H_2/C_2H_4}	α_{H_2/C_3H_6}
PPNDI	4.64	21.2	6.44	20.4	122.2	18.96	–
	(0.31)	(0.54)	(0.09)	(0.54)	(0.09)	(0.58)	
P5FPNDI	3.93 (1.55)	18.42 (1.37)	4.40 (0.70)	28.18 (1.37)	55.39 (0.70)	12.56 (3.06)	31.04 (1.24)
PB3FMPNDI	3.22	15.71	2.63	13.41	21.91	8.30	15.14
	(4.20)	(4.28)	(2.62)	(4.28)	(2.62)	(6.91)	(3.79)
P5FPONDI	3.28	14.40	3.12	20.25	42.44	13.58	34.21
	(1.08)	(1.13)	(0.54)	(1.13)	(0.54)	(1.69)	(1.32)
P5FPNDI/PPNDI	4.47	25.89	3.81	30.65	56.40	14.77	27.97
	(0.59)	(0.64)	(0.35)	(0.64)	(0.35)	(1.32)	(0.70)

branes in steady state conditions is given by

$$J = \frac{D_{eff}(C)C}{l} = \frac{P(p)P}{l} \tag{11}$$

where C and p are, respectively, the pressure and concentration of gas in the upstream chamber and in the surface of the membrane facing this chamber. From the derivative of J with respect to p, the following expression is obtained for D_{eff}

$$D_{eff}(C_i) = \left[P(p) + p\frac{\partial P(p)}{\partial p}\right]_{p_i}\left(\frac{\partial p}{\partial C}\right)_{p_i} \tag{12}$$

where C_i is the concentration of gas in the membrane at pressure p_i in the p *vs* C sorption isotherms. Eq. (12) was firstly used by Koros et al. [12] to check the reliability of the partial immobilization model. Values of D_{eff} of CO_2 and C_3H_6 are plotted as a function of the concentration in the whole pressure range in Figs. 11 and 12 for P5FPNDI and PB3FMPNDI, respectively. In the same figures and for comparative purposes the values of the diffusion coefficients obtained by the time-lag method, D_θ, are also shown. In all cases, the diffusion coefficient increases with increasing pressure, the increase being rather steeply for D_{DM} and D_{eff} at low pressures. Below the pressure at which the curve describing the variation of the permeability coefficient with pressure reaches a minimum, the values of D_{eff} and D_{DM} are in rather good agreement, but above this pressure D_{eff} continues increasing with pressure whereas D_{DM} remains practically constant because the dual-mode model no longer holds. The values of D_θ are a factor one half or lower of those corresponding to D_{eff}. The cause of this disagreement may lie in that the time-lag method used to estimate D_θ requires that the diffusion coefficient is independent on concentration.

As indicated above, the increase in the permeability coefficient of CO_2 and C_3H_6 above a certain pressure is attributed to the diffusive step. In fact membranes under high pressure of condensable gases undergo a dilation presumably coming from the penetrant in the dense regions because the gas in the rigid Langmuir sites hardly contributes to dilation [32]. If this assumption holds, the change in volume with respect to the volume at vacuum, V_0, is given by

$$\frac{\Delta V}{V_0} = \frac{k_D p\overline{V}}{22,414} \tag{13}$$

The values of $\Delta V/V_0$ can be significant for gases such as propylene and carbon dioxide. For example, the percentage of dilation of the P5FPNDI membrane under propylene at the pressure associated with minimum of the curve P *vs* p in Fig. 7 is ca. 4.8%. For CO_2 the change in the habit of the P *vs* p curve starts at a pressure of about 10 bar and the percentage of dilation of the membrane at this pressure is nearly similar to that of propylene at 3 bar. The dilation effect is not eliminated after depressurization as suggests the fact that the permeability coefficient of CO_2 at 15 bar in the P5FPNDI membrane was carried out after the experiment performed at 19 bar (⊕ symbol in Fig. 7). The same occurs with the permeability coefficient of propylene in the P5FPNDI membrane, indicated by the symbol ⊠ (in Fig. 7, obtained after the experiment performed at 8.4 bar). As a consequence of the increase in the free volume of the membranes under high pressure for highly condensable gases the distribution of transient activated gaps that favor gas transport is favored and as a result the diffusion coefficient increases at high pressures. Moreover, the original chain packaging structure is not recovered after the depressurization process. The effect of dilation on gas transport has been thoroughly studied by Coleman and Koros [32] in fluorine-containing polyimides who found that the conditioning of the membranes with CO_2 at high pressure followed by an exchange with equimolecular mixture of CO_2 and CH_4 results in an increase of the methane and a slight decrease in the permselectivity relative to the membranes prior to conditioning. This behavior was observed in the experiments carried out on membranes which had been conditioned under pressures of CO_2 and CH_4 above that ones corresponding to the minimum of the curves P *vs* p. As a result, care was taken in this work not to carry experiments at low pressures in membranes conditioned under moderately high pressures of the condensable gases used in this work.

The effect of the fluorinated moieties attached to the dicarboximide moiety of the membranes was estimated from the permselectivity coefficient given by

$$\alpha\left(\frac{A}{B}\right) = \frac{P(A)}{P(B)} \tag{14}$$

The comparison of the permselectivities of different pairs of gases in the membranes is collected in Table 6 where the numbers between brackets denote the permeability coefficient of the less permeable gas of the pair of gases considered. In general, the results show that the lower the permeability the higher the permselectivity. For example, the schematic replacement of the phenyl group in the PPNDI membrane by the perfluorinated phenyl to yield the P5FPNDI membrane increases the permeability coefficient of nitrogen in nearly 400%, in detriment of the permselectivity coefficient $\alpha(O_2/N_2)$ that decreases about 15%. In turn, the replacement of the perfluorinated phenyl group in the P5FPNDI membrane by the 3,5-bis(trifluoromethyl)phenyl moiety yielding the PB3FMPNDI membrane augments the permeability coefficient of nitrogen in the latter membrane in 170%, but decreases $\alpha(O_2/N_2)$ ca. 18%. Both the P5FPNDI and the PB3FMPNDI membrane exhibit fairly good properties to separate CO_2 from CH_4, C_2H_4 from C_2H_6 as well as H_2 from low molecular weight hydrocarbon gases. The performance of the other membranes used in this study for gases separation is lower than that of P5FPNDI and PB3FMPNDI membranes.

5. Conclusions

The presence of fluorine atoms in the substituted dicarboximide side group is more effective to increase gas permeability than the attachment of bulky moieties such as the adamantyl group to the dicarboximide group. The significant increase in the permeability of the membranes arises from the increase of both the diffusion

and the solubility coefficients caused by the C–F bonds. As a result of quadripole interactions between the CO_2 and the polar chains, the polymer–gas interaction parameter is lower for this gas than for the non-polar propylene. The significant increase of the permeability of the gases in the fluorinated membranes is accompanied by only a small decrease in gas permselectivity. The effective diffusion coefficient directly obtained from the pressure dependences of both the permeability and the gas concentration is similar to that calculated by the dual-mode model parameters but nearly two times that estimated from the time-lag method. Conditioning of the membranes under moderately high pressures of condensable gases such as carbon dioxide and propylene increases gases diffusivity.

Acknowledgments

We thank CONACyT and DGAPA-UNAM PAPIIT for generous support with contracts 23432 and ES-104307. Financial support from National Council for Science and Technology of Mexico (CONACYT) (Ph.D. Scholarship to A.A.S.) is gratefully acknowledged. We are grateful to Alejandrina Acosta, Gerardo Cedillo, Salvador López Morales, Miguel Ángel Canseco and Esteban Fregoso-Israel for their assistance in NMR, GPC and thermal properties, respectively. The authors also acknowledge financial support provided by the DGICYT (Dirección General de Investigación Científica y Tecnológica) through Grant MAT2008-06725-C03-01.

Appendix A. Supplementary data

Supplementary data associated with this article can be found, in the online version, at doi:10.1016/j.memsci.2010.06.007.

References

[1] N.R. Grove, P.A. Kohl, S.A. Bidstrup-Allen, R.A. Shick, B.L. Goodall, S. Jayaraman, Proceedings of the International Conference on Multichip Modules, IMAPS and IEEE, April 2–4, 1997, pp. 224–227.
[2] K.D. Dorkenoo, P.H. Pfromm, M.E. Rezac, Gas transport properties of a series of high Tg polynorbornenes with aliphatic pendant groups, J. Polym. Sci. B: Polym. Phys. 36 (1998) 797–803.
[3] T. Steinhäusler, W.J. Koros, Gas permeation and sorption studies on stereoregular polynorbornene, J. Polym. Sci. B: Polym. Phys. 35 (1997) 91–99.
[4] A. Pineda-Contreras, M.A. Tlenkopatchev, M. López-González, E. Riande, Synthesis and gas transport properties of new high glass transition temperature ring-opened polynorbornenes, Macromolecules 35 (2002) 4677–4684.
[5] M.A. Tlenkopatchev, J. Vargas, M. López-González, E. Riande, Gas transport in polymers prepared via metathesis copolymerization of *exo-N*-phenyl-7-oxanorbornene-5,6-dicarboximide and norbornene, Macromolecules 36 (2003) 8483–8488.
[6] J. Pozuelo, M. López-González, M. Tenklopatchev, E. Saiz, E. Riande, Simulations of gas transport in membranes based on polynorbornenes functionalized with substituted imide side groups, J. Membr. Sci. 310 (2008) 474–483.
[7] D. O'Hagan, Understanding organofluorine chemistry. An introduction to the C–F bond, Chem. Soc. Rev. 37 (2008) 308–319.
[8] Y.P. Yampol'skii, N.B. Bespalova, E.Sh. Finkel'shtein, V.I. Bondar, A.V. Popov, Synthesis, gas permeability, and gas sorption properties of fluorine-containing norbornene polymers, Macromolecules 27 (1994) 2872–2878.
[9] J Vargas, A. Martínez, A.A. Santiago, M.A. Tlenkopatchev, R. Gaviño, M. Aguilar-Vega, The effect of fluorine atoms on gas transport properties of new polynorbornene dicarboximides, J. Fluorine Chem. 130 (2009) 162–168.
[10] M.A. Tlenkopatchev, J. Vargas, M.A. Girón, M. López-González, E. Riande, Gas sorption in new fluorine containing polynorbornene with imide side chain groups, Macromolecules 38 (2005) 2696–2703.
[11] R.M. Barrer, E.K. Rideal, Permeation, diffusion and solution of gases in organic polymers, Trans. Faraday Soc. 35 (1939) 628–643.
[12] W.J. Koros, D.R. Paul, A.A. Rocha, Carbon dioxide sorption and transport in polycarbonate, J. Polym. Sci.: Polym. Phys. Ed. 14 (1976) 687–702.
[13] W.R. Vieth, J.M. Howell, J.H.J. Hsieh, Dual sorption theory, J. Membr. Sci. 1 (1976) 177–220.
[14] D.R. Paul, W.J. Koros, Effect of partially immobilizing sorption on permeability and the diffusion time lag, J. Polym. Sci.: Polym. Phys. Ed. 14 (1976) 675–685.
[15] R.E. Kesting, A.K. Fritzsche, Polmeric Gas Separation Membranes, Wiley-Interscience, New York, 1993, p. 32.
[16] S. Wu, Polymer Interface and Adhesion, Marcel Dekker, New York, 1982.
[17] Y. Kobatake, J.H. Hidelbrand, Solubility and entropy of solution of He, N_2, A, O_2, CH_4, C_2H_6, CO_2 and SF_6 in various solvents; regularity of gas solubility, Phys. Chem. 65 (1961) 331–335.
[18] H. Reiss, N.L. Frisch, E. Helfand, J.L. Lehovetz, Aspects of the statistical thermodynamics of real fluids, J. Chem. Phys. 32 (1960) 119–124.
[19] V.V. Volkov, A.K. Bokarev, V.S. Khotimskii, Proceedings of the International Symposium on Membranes and Membrane Separation Processes, Torun, Poland, 1989, p. 9.
[20] J.H. Petropoulos, Some important aspects of solubility of simple micromolecules in polymeric media, Pure Appl. Chem. 65 (1993) 219–228.
[21] M.M. López-González, V. Compañ, E. Riande, Langmuir sites in semicrystalline rubbery films? Macromolecules 36 (2003) 8576–8578.
[22] W.J. Koros, D.R. Paul, CO2 sorption in poly(ethylene terephthalate) above and below the glass transition, J. Polym. Sci.: Polym. Phys. Ed. 16 (1978) 1947–1963.
[23] N. Muruganandam, W.J. Koros, D.R. Paul, Gas sorption and transport in substituted polycarbonates, J. Polym. Sci. B: Polym. Phys. 25 (1987) 1999–2026.
[24] J.S. McHattie, W.J. Koros, D.R. Paul, Effect of isopropylidene replacement on gas transport properties polycarbonates, J. Polym. Sci. B: Polym. Phys. 29 (1991) 731–746.
[25] M. Aguilar-Vega, D.R. Paul, Gas transport properties of poly(2,2,4,4-tetramethylcyclobutane carbonate), J. Polym. Sci. B: Polym. Phys. 31 (1993) 991–1004.
[26] P. Masi, D.R. Paul, J.W. Barlow, Gas sorption and transport in a copolyester and its blend with polycarbonate, J. Polym. Sci: Polym. Phys. Ed. 20 (1982) 15–26.
[27] H. Kumazawa, J.-S. Wang, T. Fukuda, E. Sada, Permeation of carbon dioxide in glassy poly(ether imide) and poly(ether ether ketone) membranes, J. Membr. Sci. 93 (1994) 53–59.
[28] M.H. Cohen, D.J. Turnbull, Molecular transport in liquids and glasses, J. Chem. Phys. 31 (1959) 1164–1169.
[29] A. Bondi, Physical Properties of Molecular Crystals, Liquids and Glasses, Wiley, New York, 1968.
[30] D.W. van Krevelen, Properties of Polymers, Elsevier, New York, 1990.
[31] X.-Y. Wang, K.M. Lee, Y. Lu, M.T. Stone, I.C. Sanchez, B.D. Freeman, Cavity size distributions in high free volume glassy polymers by molecular simulation, Polymer 45 (2004) 3907–3912.
[32] M.R. Coleman, W.J. Koros, Conditioning of fluorine-containing polyimides. 2. Effect of conditioning protocol at 8 volume dilation on gas-transport properties, Macromolecules 32 (1999) 3106–3113.